

Mutation Scanning Using MUT-MAP, a High-Throughput, Microfluidic Chip-Based, Multi-Analyte Panel

Rajesh Patel^{1*}, Alison Tsan², Rachel Tam¹, Rupal Desai¹, Nancy Schoenbrunner², Thomas W. Myers³, Keith Bauer³, Edward Smith³, Rajiv Raja¹

1 Oncology Biomarker Development, Genentech Inc., South San Francisco, California, United States of America, **2** Chemistry and Innovation Technology, Pleasanton, California, United States of America, **3** Program in Core Research Roche Molecular Systems Inc., Pleasanton, California, United States of America

Abstract

Targeted anticancer therapies rely on the identification of patient subgroups most likely to respond to treatment. Predictive biomarkers play a key role in patient selection, while diagnostic and prognostic biomarkers expand our understanding of tumor biology, suggest treatment combinations, and facilitate discovery of novel drug targets. We have developed a high-throughput microfluidics method for mutation detection (MUT-MAP, mutation multi-analyte panel) based on TaqMan or allele-specific PCR (AS-PCR) assays. We analyzed a set of 71 mutations across six genes of therapeutic interest. The six-gene mutation panel was designed to detect the most common mutations in the *EGFR*, *KRAS*, *PIK3CA*, *NRAS*, *BRAF*, and *AKT1* oncogenes. The DNA was preamplified using custom-designed primer sets before the TaqMan/AS-PCR assays were carried out using the Biomark microfluidics system (Fluidigm; South San Francisco, CA). A cross-reactivity analysis enabled the generation of a robust automated mutation-calling algorithm which was then validated in a series of 51 cell lines and 33 FFPE clinical samples. All detected mutations were confirmed by other means. Sample input titrations confirmed the assay sensitivity with as little as 2 ng gDNA, and demonstrated excellent inter- and intra-chip reproducibility. Parallel analysis of 92 clinical trial samples was carried out using 2–100 ng genomic DNA (gDNA), allowing the simultaneous detection of multiple mutations. DNA prepared from both fresh frozen and formalin-fixed, paraffin-embedded (FFPE) samples were used, and the analysis was routinely completed in 2–3 days: traditional assays require 0.5–1 µg high-quality DNA, and take significantly longer to analyze. This assay can detect a wide range of mutations in therapeutically relevant genes from very small amounts of sample DNA. As such, the mutation assay developed is a valuable tool for high-throughput biomarker discovery and validation in personalized medicine and cancer drug development.

Citation: Patel R, Tsan A, Tam R, Desai R, Schoenbrunner N, et al. (2012) Mutation Scanning Using MUT-MAP, a High-Throughput, Microfluidic Chip-Based, Multi-Analyte Panel. PLoS ONE 7(12): e51153. doi:10.1371/journal.pone.0051153

Editor: Todd W. Miller, Dartmouth, United States of America

Received: August 22, 2012; **Accepted:** October 17, 2012; **Published:** December 17, 2012

Copyright: © 2012 Patel et al. This is an open-access article distributed under the terms of the Creative Commons Attribution License, which permits unrestricted use, distribution, and reproduction in any medium, provided the original author and source are credited.

Funding: This study was funded by Genentech Inc. The funders were responsible for the study design, data collection and analysis, decision to publish, and preparation of the manuscript.

Competing Interests: The authors have the following interests: All studies were funded by Genentech, Inc. Support for third-party writing assistance for this manuscript was provided by Genentech, Inc. Rajesh Patel, Rachel Tam, Rupal Desai and Rajiv Raja are or were employed by Genentech and Alison Tsan, Nancy Schoenbrunner Thomas W. Myers, Keith Bauer and Edward Smith are or were employed by Roche Molecular Systems Inc. There are no patents, products in development or marketed products to declare. This does not alter the authors' adherence to all the PLOS ONE policies on sharing data and materials.

* E-mail: rajeshdp@gene.com

Introduction

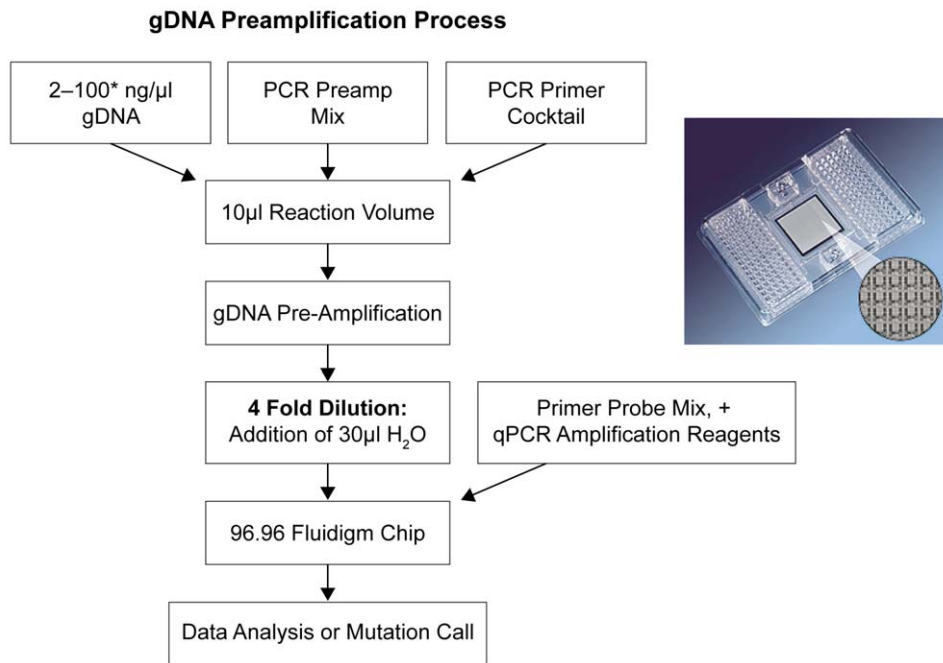
Biomarkers have assumed a central role in oncology, enabling the detection, characterization, and targeted treatment of a range of cancer types [1]. The successful application of targeted anticancer therapies depends on the detection of disease subtypes that are most likely to respond to treatment. As such, the detection and validation of tumor biomarkers is critical for the ongoing development of personalized healthcare, both through the support of effective and robust drug trials, and the effective employment of targeted therapies in the clinic [2].

Biomarkers are classified according to their utility: diagnostic biomarkers are indicators of biological status that allow classification of tumors according to their genetic and/or phenotypic characteristics. Predictive biomarkers allow the response to a particular line of treatment to be anticipated, based on the known mode of action of the chosen therapy and an understanding of the underlying tumor biology. Prognostic biomarkers enable the prediction of disease progression in the absence of treatment,

and have been used to identify signaling pathways that are potential drivers of disease, and putative drug targets [3].

Although techniques such as tissue microarray immunohistochemistry (IHC) and reverse-transcription polymerase chain reaction (RT-PCR) allow high-throughput screening of protein and mRNA biomarkers in clinical samples [4], significant challenges remain. Biomarker levels vary across human populations, and significant heterogeneity may be observed within single cancer types, even within samples from a single tumor [5,6]. This is exacerbated by the possibility that first-line chemotherapy may induce DNA damage in tumor cells, leading to changes in biomarker status; as biopsy samples are often obtained before first-line treatment, this may be an obstacle to the correct selection of subsequent targeted therapies, although the extent of this effect remains unclear [6].

While some anticancer therapeutics are entering the clinic with companion diagnostic tests, a wider characterization of tumor gene expression and mutation status will enable targeted therapies



*Based on quality of DNA

Figure 1. High-Throughput Mutation Detection, Workflow, and Protocol.
doi:10.1371/journal.pone.0051153.g001

Table 1. Mutation Coverage Breakdown by Gene.

Six-Gene Mutation Coverage by TaqMan and Prototype <i>EGFR</i> and <i>KRAS</i> AS-PCR Assays						
Gene	Mutation Count	Exon	Mutation ID	cDNA Mutation Position	Amino Acid Mutation Position	
<i>EGFR</i>	43	18	6252	2155 G>A	G719S	
			6253	2155 G>T	G719C	
			6239	2156 G>C	G719A	
			19	See table 2 for EGFR exon 19 deletion mutation coverage		
			20	6241	2303 G>T	S768I
		12376		2307_2308 ins 9(gccagcgtg)	V769_D770insASV	
		13558		2309_2310 complex(ac>ccagcgtggat)	V769_D770insASV	
		12378		2310_2311 ins GGT	D770_N771insG	
		13428		2311_2312 ins 9(gcgtggaca)	D770_N771insSVD	
		12377		2319_2320 ins CAC	H773_V774insH	
		6240		2369 C>T	T790M	
				21	6224	2573 T>G
		12429	2573-2574 TG>GT		L858R	
	6213	2582 T>A	L861Q			
<i>PIK3CA</i>	4	9	760	1624 G>A	E542K	
			763	1633 G>A	E545K	
			20	775	3140 A>G	H1047L
		776		3140 A>T	H1047R	
<i>KRAS</i>	18	2	522	35 G>C	G12A	

Table 1. Cont.

Six-Gene Mutation Coverage by TaqMan and Prototype <i>EGFR</i> and <i>KRAS</i> AS-PCR Assays					
Gene	Mutation Count	Exon	Mutation ID	cDNA Mutation Position	Amino Acid Mutation Position
			516	34 G>T	G12C
			521	35 G>A	G12D
			517	34 G>A	G12S
			518	34 G>C	G12R
			520	35 G>T	G12V
			512	34_35 GG>TT	G13D
			532	38 G>A	G12F
			533	38 G>C	G13A
			527	37 G>T	G13C
			529	37 G>C	G13R
			528	37 G>A	G13S
			534	38 G>T	G13V
		3	554	183 A>C	Q61H
			555	183 A>T	Q61H
			549	181 C>A	Q61K
			553	182 A>T	Q61L
			552	182 A>G	Q61R
<i>BRAF</i>	1	15	476	1799 T>A	p.V600E
<i>NRAS</i>	4	2	564	38 G>A	p.G13D
			580	181 C>A	p.Q61K
		3	584	182 A>G	p.Q61R
			583	182 A>T	p.Q61L
<i>AKT1</i>	1	4	33765	49 G>A	p.E17K

doi:10.1371/journal.pone.0051153.t001

to be combined for specific patient groups without multiple biopsy procedures. A deeper understanding of different tumor subtypes will help explain mechanisms of drug resistance and open up new channels of therapy and research. For this reason, “biomarker pipelines” play an important role in the development of molecular targeted therapies [7].

There are additional challenges associated with biomarker identification using clinical samples containing poor-quality or degraded DNA in limited quantities. Most clinical samples are formalin fixed and paraffin embedded (FFPE) for preservation and storage. While enabling samples to be archived for subsequent biomarker identification and comparison with patient outcomes, this method of preservation leads to nucleic acid fragmentation and cross-linking, so only a small proportion of sample DNA can be probed successfully [8]. Traditional methods of biomarker detection require 0.5–1 µg high-quality DNA and results may take a significant amount of time to analyze, particularly if samples are to be screened for multiple mutations.

We have developed a high-throughput method for mutation detection (MUT-MAP, mutation multi-analyte panel) based on TaqMan and allele-specific PCR (AS-PCR) assays using a microfluidic chip-based technology. This approach allows the rapid analysis of 71 mutations across a panel of six genes of therapeutic interest. Parallel analysis of 92 clinical trial samples can be carried out using miniscule amounts of DNA (2–100 ng,

based on the quality of genomic DNA [gDNA] isolated), allowing the simultaneous detection of multiple mutations in a single sample. DNA can be isolated from both fresh frozen and FFPE samples, and the analysis is routinely completed in 2–3 days.

The six-gene panel mutation assay was designed to detect the most common mutations found in *EGFR*, *KRAS*, *PIK3CA*, *NRAS*, *BRAF*, and *AKT1*. Activating mutations in these genes cause aberrant cell signaling and are found in various types of cancer; their encoded proteins are therefore targets for therapeutic inhibition. For example, mutations in *EGFR* are linked with increased activation of the epidermal growth factor receptor (EGFR) signaling pathway, which drives tumor growth and promotes survival in several types of cancer [9]. The *EGFR* and *KRAS* mutation status is predictive of response to anti-EGFR-targeted therapies such as erlotinib, gefitinib [10], and cetuximab [11]. Additionally, the *BRAF* inhibitor vemurafenib is only effective in patients with *V600* mutation-positive melanoma [12,13], and the phosphoinositide-3-kinase (PI3K) inhibitor GDC-0941 is most effective in preclinical tumor models with *PIK3CA* mutations [14].

Although next-generation parallel sequencing holds great promise for mutation detection across the whole genome, these technologies are not yet mature enough for routine, high-throughput analysis of precious clinical samples. Parallel sequencing generally requires larger quantities of DNA for analysis and

Table 2. Mutation Coverage for EGFR Exon 19 Deletions.

EGFR Exon 19 Deletion Mutations Covered by Prototype EGFR AS-PCR Assays			
Mutation Count	Mutation ID	cDNA Mutation Position	Amino Acid Mutation Position
30	26038	2233_2247del15	K745_E749del
	13550	2235_2248>AATTC	E746_A750>IP
	6223	2235_2249del15	E746_A750del
	13552	2235_2251>AATTC	E746_T751>IP
	13551	2235_2252>AAT	E746_T751>I
	12385	2235_2255>AAT	E746_S752>I
	12413	2236_2248>AGAC	E746_A750>RP
	6225	2236_2250del15	E746_A750del
	12728	2236_2253del18	E746_T751del
	12678	2237_2251del15	E746_T751>A
	12386	2237_2252>T	E746_T751>V
	12416	2237_2253>TTGCT	E746_T751>VA
	12367	2237_2254del18	E746_S752>A
	12384	2237_2255>T	E746_S752>V
	18427	2237_2257>TCT	E746_P753>VS
	12422	2238_2248>GC	L747_A750>P
	23571	2238_2252del15	L747_T751del
	12419	2238_2252>GCA	L747_T751>Q
	6220	2238_2255del18	E746_S752>D
	6218	2239_2247del9	L747_E749del
	12382	2239_2248TTAAGAGAAG>C	L747_A750>P
	12383	2239_2251>C	L747_T751>P
	6254	2239_2253del15	L747_T751del
	6255	2239_2256del18	L747_S752del
	12403	2239_2256>CAA	L747_S752>Q
	12387	2239_2258>CA	L747_P753>Q
	6210	2240_2251del12	L747_T751>S
	12369	2240_2254del15	L747_T751del
	12370	2240_2257del18	L747_P753>S
	13556	2253_2276del24	S752_I759del

doi:10.1371/journal.pone.0051153.t002

takes longer to generate data in comparison with our approach. The MUT-MAP microfluidics system provides a readily available platform for the exploratory detection of predictive and prognostic biomarkers in support of current and future personalized healthcare.

Materials and Methods

Overview of the MUT-MAP Microfluidics System

Mutation screening with the MUT-MAP microfluidics system is a multi-stage process. First, DNA is preamplified using custom-designed primer sets for the exons/genes of interest. The BioMark platform (Fluidigm Corp.) is then used to conduct a combination of quantitative PCR (qPCR) mutation detection assays. We employ two assay formats for mutation detection: both formats utilize TaqMan detection of the amplified product [15]. In one format, which we refer to as TaqMan genotyping or, simply, TaqMan, the discrimination between mutant and wild-type is driven by a differentially-labeled mutant- and wild-type-specific

probe [16]. In the other assay format, the discrimination is driven by a mutant-specific primer, or allele-specific PCR (AS-PCR [17,18]). The AS-PCR assays incorporate the use of an engineered *Thermus* species Z05 DNA polymerase (AS1) and, in some cases, covalently modified primers to enhance the specificity of allele-specific qPCR [19,20].

The AS-PCR assays were used for *KRAS* and *EGFR* mutation analysis, and have broader coverage of the predominant mutations in these two genes compared with some commercially available assays. An overview of the protocol and process flow is presented in figure 1.

The BioMark protocol involves the introduction of premixed qPCR reagents and preamplified DNA onto the MUT-MAP assay chip via the sample inlets. Assay-specific TaqMan primer/probe mixes are normally added via assay ports. This protocol was modified due to the presence of primers and probes in the qPCR reagents for some reactions (EGFR Mutation Test; Roche Molecular Systems, Inc. [RMS]; Pleasanton, CA). To ensure compatibility with the BioMark platform, these samples were

Table 3. Cross-Reactivity of *AKT1*, *BRAF*, *PIK3CA*, and *NRAS* Mutants.

Assays	Plasmid controls <i>AKT1</i> , <i>BRAF</i> , <i>PIK3CA</i> , and <i>NRAS</i>										Controls	
	Ak_E17K	Br_V600E	Pk_E542K	Pk_E545K	Pk_H1047R	Pk_H1047L	Nr_Q61K	Nr_Q61R	Nr_Q61L	Nr_G12D	gDNA	NTC
RNaseP	30.0	30.0	30.0	30.0	30.0	30.0	30.0	30.0	30.0	30.0	11.5	30.0
AKT_WT	30.0	30.0	30.0	30.0	30.0	30.0	30.0	30.0	30.0	30.0	15.8	30.0
AKT_E17K	20.0	30.0	30.0	30.0	30.0	30.0	30.0	30.0	30.0	30.0	30.0	30.0
Br_WT	30.0	30.0	30.0	30.0	30.0	30.0	30.0	30.0	30.0	30.0	13.1	30.0
Br_V600E	30.0	22.4	30.0	30.0	30.0	30.0	30.0	30.0	30.0	30.0	30.0	30.0
Pk_E542_WT	30.0	30.0	30.0	20.6	30.0	30.0	30.0	30.0	30.0	30.0	15.5	30.0
Pk_E542K	30.0	30.0	16.6	30.0	30.0	30.0	30.0	30.0	30.0	30.0	30.0	30.0
Pk_E545_WT	30.0	30.0	15.3 ^a	30.0	30.0	30.0	30.0	30.0	30.0	30.0	12.9	30.0
Pk_E545K	30.0	30.0	30.0	17.2	30.0	30.0	30.0	30.0	30.0	30.0	30.0	30.0
Pk_H1047_WT	30.0	30.0	30.0	30.0	30.0	20.0	30.0	30.0	30.0	30.0	12.0	30.0
Pk_H1047R	30.0	30.0	30.0	30.0	15.7	19.1 ^a	30.0	30.0	30.0	30.0	30.0	30.0
Pk_H1047_WT	30.0	30.0	30.0	30.0	30.0	26.5	30.0	30.0	30.0	30.0	12.1	30.0
Pk_H1047L	30.0	30.0	30.0	30.0	30.0	16.9	30.0	30.0	30.0	30.0	30.0	30.0
Nr_Q61_WT	30.0	30.0	30.0	30.0	30.0	30.0	30.0	30.0	30.0	30.0	10.5	30.0
Nr_Q61K	30.0	30.0	30.0	30.0	30.0	30.0	19.1	30.0	30.0	30.0	30.0	30.0
Nr_Q61_WT	30.0	30.0	30.0	30.0	30.0	30.0	30.0	30.0	30.0	30.0	10.6	30.0
Nr_Q61R	30.0	30.0	30.0	30.0	30.0	30.0	30.0	22.0	30.0	30.0	30.0	30.0
Nr_Q61_WT	30.0	30.0	30.0	30.0	30.0	30.0	30.0	30.0	30.0	30.0	10.6	30.0
Nr_Q61L	30.0	30.0	30.0	30.0	30.0	30.0	30.0	30.0	17.1	30.0	30.0	30.0
Nr_G12_WT	30.0	30.0	30.0	30.0	30.0	30.0	30.0	30.0	30.0	16.2 ^a	10.5	30.0
Nr_G12D	30.0	30.0	30.0	30.0	30.0	30.0	30.0	30.0	30.0	16.7	30.0	30.0

^aCross-reactions between the assays are unidirectional and hence do not interfere with accurate mutation calls.
doi:10.1371/journal.pone.0051153.t003

introduced via the assay inlets, and both TaqMan and AS-PCR assay reagents were added via the sample inlets on the microfluidic chip. Data analysis was also modified to accommodate these changes.

DNA Preamplification

DNA was preamplified in 10 µl reactions on a 96-well plate using a preamplification primer cocktail (Table S1) in the presence of 1x ABI PreAmp Master Mix (Applied Biosystems; Foster City, CA). gDNA (2–10 ng) was isolated from cell lines and fresh frozen samples. However, due to the poor quality of DNA obtained from FFPE clinical samples, 50–100 ng was used for preamplification from this source. Primer concentrations were 100 nM during the amplification reaction. Each preamplification sample set included a gDNA control to determine preamplification performance as well as a no-template control. An additional positive control was made in bulk by preamplification of a cocktail of relevant mutant plasmids for all six genes; this control was run on every chip.

Samples were preamplified using a Tetrad Thermal Cycler (BioRad; Hercules, CA) according to the following protocol: 95°C for 10 minutes, then thermal cycling (20 cycles, each of 15 seconds at 95°C followed by 2 minutes at 60°C). Samples were diluted fourfold, mixed, centrifuged at 3500 rpm (5810 R; Eppendorf; Hauppauge, NY), and stored at 4°C or –20°C until further processing. Following preamplification, rigorous procedures were followed to prevent sample contamination, including the use of dedicated workspaces and pipettes for pre- and post-

PCR reaction set-up, laminar flow hoods, and personal protective equipment.

Preparation of Reagents

Primer/probe concentrations of 900/200 nM were used in the TaqMan reactions to detect mutations in the *PIK3CA*, *BRAF*, *NRAS*, and *AKT* genes. Custom AS-PCR assays (Roche Molecular Systems) were used to detect mutations in *KRAS* and *EGFR* genes along with custom wild-type assays for both genes. A complete description of primers and probes for the TaqMan reactions is presented in table S2.

A commercially available EGFR Mutation Test (Roche Molecular Systems) was modified to achieve compatibility with the two-color BioMark readout (FAM and VIC) for detection of mutations in *EGFR*. Hexachlorofluorescein (HEX)-labeled probes were spiked into kit mastermixes to detect *S768I* and *T790M* in the VIC channel. Additionally, a custom fourth tube was designed to separately detect exon 20 insertion mutations using MMX3 from the RMS EGFR Mutation Test. The *KRAS* allele-specific assays utilized a research kit from Roche Molecular Systems.

Both TaqMan and AS-PCR assays were carried out using the AS1 qPCR master mix. Rox dye (final concentration 55 nM) for signal normalization and 20x gel electrophoresis sample loading buffer (Fluidigm Corp.) were added to the qPCR reactions.

Assays along with AS1 qPCR master mix were run in duplicate by loading 5 µl into each well of the primed 96.96 Fluidigm Chip. The diluted preamplified DNA samples were mixed with equal volumes of 2x DNA assay loading buffer (Fluidigm Corp.). The samples were run by loading 5 µl into each well on the chip. The

Table 4. Cross-Reactivity of KRAS Mutants.

Assays	Plasmid Controls KRAS																Controls								
	Kr_G12S	Kr_G12C	Kr_G12R	Kr_G12D	Kr_G12V	Kr_G12A	Kr_G12A	Kr_G12V	Kr_G12D	Kr_G12R	Kr_G12C	Kr_G12S	Kr_G13C	Kr_G13R	Kr_G13D	Kr_G13V	Kr_G13A	Kr_Q61K	Kr_Q61L	Kr_Q61R	Kr_Q61Hc	Kr_Q61Ht	gDNA	NTC	
Kr_cntrl	12.1	12.2	12.1	12.0	12.1	12.4	13.1	12.5	12.6	12.0	13.3	11.6	12.3	12.9	12.4	12.6	13.0	12.9	12.4	12.6	13.0	12.9	10.4	30.0	30.0
Kr_G12S	14.3	24.8	28.0	28.3	26.6	25.7	30.0	25.8	27.7	26.1	26.4	25.7	25.8	24.2	24.6	24.7	26.7	27.3	23.9	23.9	26.7	27.3	23.9	30.0	30.0
Kr_G12C	24.9	14.6	24.2	29.4	27.9	29.1	17.6 ^a	26.9	28.9	27.9	30.0	30.0	29.6	26.4	28.7	28.9	28.5	30.0	25.6	30.0	28.5	30.0	25.6	30.0	30.0
Kr_G12R	28.7	24.2	14.2	29.8	30.0	28.2	30.0	30.0	28.9	26.0	30.0	28.2	30.0	28.4	30.0	29.4	29.0	28.3	28.5	30.0	29.0	28.3	28.5	30.0	30.0
Kr_G12D	27.6	28.5	23.8	13.6	24.8	28.1	30.0	25.2	25.2	24.5	25.3	24.9	25.7	25.0	24.8	25.0	25.9	27.4	22.9	30.0	29.0	28.3	28.5	30.0	30.0
Kr_G12V	18.2	23.4	25.8	13.7 ^a	13.8	22.7	20.3	24.2	24.3	24.8	23.5	23.9	22.9	22.6	23.3	23.1	23.8	23.4	21.0	30.0	29.0	28.3	28.5	30.0	30.0
Kr_G12A	27.4	26.2	21.8	25.0	22.8	14.1	30.0	28.6	30.0	24.8	27.1	28.7	26.9	28.6	28.4	27.6	28.1	29.6	25.3	30.0	29.0	28.3	28.5	30.0	30.0
Kr_G12F	30.0	23.4	30.0	30.0	20.0	29.3	13.1	30.0	30.0	30.0	30.0	30.0	30.0	28.3	30.0	29.3	30.0	29.8	30.0	30.0	29.8	29.8	29.8	30.0	30.0
Kr_G13S	15.8 ^a	22.9	22.1	24.5	22.1	25.0	26.4	13.3	23.8	24.7	24.0	22.7	22.9	23.3	23.0	22.8	24.4	24.2	21.4	30.0	29.0	28.3	28.5	30.0	30.0
Kr_G13C	17.3	24.8	24.7	22.4	13.0 ^a	22.0	24.1	23.8	13.3	22.4	23.9	23.7	23.7	22.7	22.4	23.0	23.1	23.1	20.5	30.0	29.0	28.3	28.5	30.0	30.0
Kr_G13R	24.9	26.6	29.9	27.7	23.3	28.0	29.8	25.9	22.6	13.3	28.0	16.9	26.5	30.0	28.6	30.0	28.5	30.0	26.5	30.0	29.0	28.3	28.5	30.0	30.0
Kr_G13D	29.4	29.0	28.2	19.9	23.7	23.9	30.0	30.0	29.1	29.9	15.0	25.4	28.1	22.8	22.8	23.3	23.7	23.6	21.4	30.0	29.0	28.3	28.5	30.0	30.0
Kr_G13V	25.5	20.5	26.0	18.5	25.8	26.8	28.0	29.3	24.8	30.0	24.3	12.9	20.2	26.2	25.9	25.0	26.7	26.1	23.9	30.0	29.0	28.3	28.5	30.0	30.0
Kr_G13A	23.6	22.1	23.4	17.0	20.2	20.5	24.7	21.6	13.9 ^a	20.0	26.7	21.7	12.9	21.5	21.3	21.4	22.0	21.9	19.5	30.0	29.0	28.3	28.5	30.0	30.0
Kr_Q61K	26.7	27.8	27.4	26.6	27.3	26.5	27.9	25.5	27.5	25.0	29.1	25.2	25.8	15.9	30.0	30.0	30.0	25.3	30.0	30.0	29.8	29.8	29.8	30.0	30.0
Kr_Q61L	28.2	28.9	27.3	26.3	28.0	28.4	28.3	26.8	27.9	27.1	29.9	26.4	27.4	28.7	16.5	28.6	30.0	29.8	25.4	30.0	29.8	29.8	29.8	30.0	30.0
Kr_Q61R	26.4	26.8	26.8	27.0	27.2	27.4	26.4	25.3	27.3	25.1	28.3	24.6	25.3	28.5	23.6	15.4	27.8	27.0	24.2	30.0	29.8	29.8	29.8	30.0	30.0
Kr_Q61Hc	30.0	30.0	29.5	29.6	30.0	30.0	29.6	29.7	30.0	29.3	30.0	29.3	30.0	30.0	30.0	26.6	17.1	26.6	27.5	30.0	29.8	29.8	29.8	30.0	30.0
Kr_Q61Ht	28.0	27.4	29.2	27.1	27.0	29.5	28.0	26.2	28.4	25.4	29.6	25.6	25.9	26.8	28.4	26.5	28.8	16.0	24.8	30.0	29.8	29.8	29.8	30.0	30.0

^aCross-reactions between the assays are unidirectional and hence do not interfere with accurate mutation calls.
doi:10.1371/journal.pone.0051153.t004

Table 5. Cross-Reactivity of *EGFR* Mutants.

Assays	Plasmid Controls <i>EGFR</i>								Controls	
	Eg_ex28	Eg_19del	Eg_S768I	Eg_L858R	Eg_T790M	Eg_L861Q	Eg_G719X	Eg_ins	gDNA	NTC
Eg_ex20_Cntrl	30.0	30.0	15.2	30.0	17.4	30.0	30.0	14.1	11.8	30.0
Eg_ex28_Cntrl	13.0	30.0	30.0	30.0	30.0	30.0	30.0	30.0	10.1	30.0
Eg_19del	30.0	13.6	30.0	30.0	30.0	30.0	30.0	30.0	24.0	30.0
Eg_S768I	30.0	30.0	15.0	30.0	30.0	30.0	30.0	28.9	26.4	30.0
Eg_L858R	30.0	30.0	30.0	18.1	30.0	30.0	30.0	30.0	27.3	30.0
Eg_T790M	30.0	30.0	24.8	30.0	17.1	30.0	30.0	30.0	23.0	30.0
Eg_L861Q	30.0	30.0	30.0	26.1	30.0	15.7	30.0	30.0	23.2	30.0
Eg_G719X	30.0	30.0	30.0	30.0	30.0	30.0	18.5	30.0	26.5	30.0
Eg_ins	30.0	30.0	30.0	30.0	29.5	30.0	30.0	13.3	23.0	30.0

Eg_ex20_Cntrl assay detects exon 20. Hence *EGFR* exon 20 plasmids carrying *S768I*, *T790M*, and insertion mutations are detected.
doi:10.1371/journal.pone.0051153.t005

chip was then placed in the integrated fluidic circuit controller and loaded before analysis with the BioMark reader. The following thermal cycling protocol was used: 50°C (2 minutes), 70°C (30 minutes), 25°C (10 min), 50°C (2 minutes), and 95°C (4 minutes). This was followed by 40 cycles of 95°C (10 seconds) and 61°C (30 seconds). The initial cycle [50°C (2 minutes), 70°C (30 minutes), 25°C (10 minutes)] is part of the protocol recommended by Fluidigm for the 96.96 chip to ensure sufficient mixing of the reagents.

Data were analyzed and cycle threshold (C_T) values were determined using BioMark real-time PCR analysis software (Fluidigm Corp.), and automated mutation calling was carried out using an algorithm based on the change in C_T (ΔC_T) values between wild-type and mutant or between control and mutant, for TaqMan and AS-PCR assays, respectively.

Six-Gene Mutation Panel

The use of MUT-MAP in this study allowed the screening of 71 mutations across the *EGFR*, *KRAS*, *PIK3CA*, *NRAS*, *BRAF*, and *AKT1* genes. The mutation coverage of this panel is presented in tables 1 and 2. Validation of mutations detected in clinical samples was performed using commercial mutation detection assays (Qiagen DxS assays for *PIK3CA*, *KRAS*, and *EGFR* mutations), and in-house developed and validated TaqMan assays (for *BRAF*, *NRAS*, and *AKT1*).

Results

Plasmid Validation

A series of validation experiments was carried out to confirm the reproducibility and accuracy of the microfluidic assay panel. In order to validate the discrimination of closely related sequences by the mutation screening panel, a complete cross-reactivity analysis was conducted by screening every mutant plasmid target against every mutant-specific assay. The C_T values were generated by the BioMark real-time PCR analysis software (Fluidigm Corp.) and plotted as shown in tables 3, 4, and 5. A C_T value of 30.0 represents no reactivity, and is indicative of the absence of that allele from the sample. Deviations from this baseline represent assay reactivity, with a lower C_T value indicative of increased reactivity. The C_T values generated by mutant-specific assays on their corresponding mutant plasmid targets are highlighted in boxed cells (Tables 3, 4, and 5).

The C_T values and cross-reactivities obtained from the plasmid data were instrumental in generating an automated mutation-calling algorithm to detect the presence or absence of mutations in clinical samples for each of the six genes in the panel. Samples were re-run on multiple chips to validate both intra- and inter-chip reproducibility.

In general, all samples were correctly identified with high reproducibility and no confounding cross-reactivity. Where cross-reactivity did occur, it was generally an easily discriminated partial reaction. For example, in the TaqMan assays, the cross-reactivity observed between alleles such as *PIK3CA E545* wild-type and *E542K* can be attributed to cross-reactivity of probes with highly similar sequences. In the *KRAS* AS-PCR assays, cross-reactivity is likely due to sequence content at the 3' end of the primer sequences. The unidirectional nature of these cross-reactions made it easy to build an algorithm to classify mutation status.

Validation of Cell Line Samples

For cell lines and clinical samples, gene-specific custom algorithms were written, taking into account the control C_T and the mutant C_T values. Samples showing $\Delta C_T < 6$ were classified as positive for the specific mutation.

A series of 51 cell lines was screened to detect mutations across the six genes (Table 6). These mutation calls were compared with published characteristics of these cell lines, from the Catalogue of Somatic Mutations in Cancer (COSMIC) [21].

Validation with FFPE Samples

The assay was further validated using clinical FFPE samples harboring known mutations in the genes of interest. A series of 33 FFPE tumor biopsy samples were analyzed by the six-gene mutation panel. Results were compared with data from traditional micro-well plate qPCR assays: mutations in *EGFR*, *KRAS*, and *PIK3CA* were confirmed using Qiagen DxS assays whereas mutations in *BRAF*, *NRAS*, and *AKT1* were validated with custom in-house-validated TaqMan assays. Execution of the experiments was notably faster with the multiplex assay than with the traditional methods. The MUT-MAP system also required only 20–100 ng DNA compared with 0.5–1 µg DNA for traditional assays (Qiagen DxS assays) covering the same set of mutations.

A good correlation was observed between the experimental results and the traditional mutation detection assays (Table 7). Where samples were available, all outputs were in agreement. The

Table 6. Correlation Between Mutation Calls in Cell Lines and Those Reported in the Literature.

Cosmic ID	Samples	Six-Gene Mutation Panel					
		<i>AKT1</i>	<i>BRAF</i>	<i>PIK3CA</i>	<i>NRAS</i>	<i>KRAS</i>	<i>EGFR</i>
1286013	MGH-U3	E17K	MND	MND	MND	MND	MND
905954	SK-MEL-28	MND	V600E	MND	MND	MND	MND
909747	SW1417	MND	V600E	MND	MND	MND	MND
905988	MDA-MB-435	MND	V600E	MND	MND	MND	MND
906844	DU4475	MND	V600E	MND	MND	MND	MND
908125	MEL-JUSO	MND	MND	MND	Q61L	MND	MND
910926	BFTC	MND	MND	MND	Q61L	MND	MND
724831	H1299	MND	MND	MND	Q61K	MND	MND
905955	SKMEL-2	MND	MND	MND	Q61R	MND	MND
909771	THP-1	MND	MND	MND	G12D	MND	MND
1018466	BT483	MND	MND	E542K	MND	MND	MND
905946	MCF-7	MND	MND	E545K	MND	MND	MND
908121	MDA-MB-361	MND	MND	E545K	MND	MND	MND
906851	EFM19	MND	MND	H1047L	MND	MND	MND
905945	T-47D	MND	MND	H1047R	MND	MND	MND
905945	T-47D	MND	MND	H1047R	MND	MND	MND
910948	MFM-223	MND	MND	H1047R	MND	MND	MND
908122	MDA-MB-453	MND	MND	H1047R	MND	MND	MND
909778	UACC-893	MND	MND	H1047R	MND	MND	MND
1479574	LS180	MND	MND	H1047R	MND	G12D	MND
905949	A549	MND	MND	MND	MND	G12S	MND
905942	NCI-H23	MND	MND	MND	MND	G12C	MND
910546	PSN-1	MND	MND	MND	MND	G12R	MND
910702	AsPC-1	MND	MND	MND	MND	G12D	MND
908122	SW403	MND	MND	MND	MND	G12V	MND
753624	CAPAN-1	MND	MND	MND	MND	G12V	MND
724873	NCI-H2009	MND	MND	MND	MND	G12A	MND
907790	LoVo	MND	MND	MND	MND	G13D	MND
905960	MDA-MB-231	MND	MND	MND	MND	G13D	MND
907790	LOVO	MND	MND	MND	MND	G13D	MND
687800	NCI-H1650	MND	MND	MND	MND	MND	19del
1028938	HCC4006	MND	MND	MND	MND	MND	19del
1028936	HCC827	MND	MND	MND	MND	MND	19del
1336875	pC9	MND	MND	MND	MND	MND	19del
924244	NCI-H1975	MND	MND	MND	MND	MND	L858R/T790M
909751	SW48	MND	MND	MND	MND	MND	G719X
905934	PC-3	MND	MND	MND	MND	MND	MND
910781	AN3 CA	MND	MND	MND	MND	MND	MND
687804	NCI-H1770	MND	MND	MND	MND	MND	MND
905947	786-O	MND	MND	MND	MND	MND	MND
908471	NCI-H1581	MND	MND	MND	MND	MND	MND
908481	NCI-H2196	MND	MND	MND	MND	MND	MND
909907	ZR-75-30	MND	MND	MND	MND	MND	MND
688015	NCI-H2171	MND	MND	MND	MND	MND	MND
905986	SF-268	MND	MND	MND	MND	MND	MND
749712	HCC1395	MND	MND	MND	MND	MND	MND
749714	HCC1937	MND	MND	MND	MND	MND	MND

MND, mutation not detected.

doi:10.1371/journal.pone.0051153.t006

Table 7. Correlation Between Mutation Calls in FFPE Samples and Those Determined by TaqMan/Qiagen DxS Assays.

Samples	Tissues	Six-Gene Mutation Panel						TaqMan/Qiagen DxS					
		<i>AKT1</i>	<i>BRAF</i>	<i>PIK3CA</i>	<i>NRAS</i>	<i>KRAS</i>	<i>EGFR</i>	<i>AKT1</i>	<i>BRAF</i>	<i>PIK3CA</i>	<i>NRAS</i>	<i>KRAS</i>	<i>EGFR</i>
HP-40263	CO	MND	V600E	H1047R	MND	MND	MND	MND	V600E	_a	MND	MND	MND
HP-41677	CO	E17K	V600E	MND	MND	MND	MND	_a	V600E	MND	MND	MND	MND
HP-30630	CO	MND	V600E	E542K	MND	MND	MND	MND	_a	E542K	MND	MND	MND
HP-29630	CO	MND	V600E	E545K	MND	MND	MND	MND	_a	E545K	MND	MND	MND
HP-31183	NOS	MND	MND	E545K	MND	Q61R	MND	MND	MND	E545K	MND	_a	MND
HP-32064	NOS	MND	MND	H1047R	MND	G12D	MND	MND	MND	H1047R	MND	G12D	MND
HP-33002	NOS	MND	MND	E545K	MND	G12C	MND	MND	MND	E545K	MND	G12C	MND
HP-30760	NOS	MND	MND	E545K	MND	G12S	MND	MND	MND	E545K	MND	G12S	MND
HP-30626	CO	MND	MND	E542K	MND	G12V	MND	MND	MND	E542K	MND	G12V	MND
HP-40224	CO	MND	MND	MND	Q61R	MND	MND	MND	MND	MND	Q61R	MND	MND
HP-41675	CO	MND	MND	MND	Q61K	MND	MND	MND	MND	MND	Q61K	MND	MND
HP-40253	CO	MND	MND	MND	MND	G12A	MND	MND	MND	MND	MND	G12A	MND
HP-32864	NOS	MND	MND	MND	MND	G12C	MND	MND	MND	MND	MND	G12C	MND
HP-44508	CO	MND	MND	MND	MND	G12D	MND	MND	MND	MND	MND	G12D	MND
HP-40092	CO	MND	MND	MND	MND	G12D	MND	MND	MND	MND	MND	G12D	MND
HP-30770	NOS	MND	MND	MND	MND	G12R	MND	MND	MND	MND	MND	G12R	MND
HP-41699	CO	MND	MND	MND	MND	G12C	MND	MND	MND	MND	MND	G12C	MND
HP-32201	NOS	MND	MND	MND	MND	G12C	MND	MND	MND	MND	MND	G12C	MND
HP-41676	CO	MND	MND	E545K	MND	G12S	MND	MND	MND	_a	MND	G12S	MND
HP-40264	CO	MND	MND	MND	MND	G12S	MND	MND	MND	MND	MND	G12S	MND
HP-40122	CO	MND	MND	MND	MND	G12V	MND	MND	MND	MND	MND	G12V	MND
HP-41713	CO	MND	MND	MND	MND	G12V	MND	MND	MND	MND	MND	G12V	MND
HP-40249	CO	MND	MND	MND	MND	G13D	MND	MND	MND	MND	MND	G13D	MND
HP-32375	NOS	MND	MND	MND	MND	G13D	MND	MND	MND	MND	MND	G13D	MND
HP-45416	LU	MND	MND	MND	MND	MND	L858R/ T790M	MND	MND	MND	MND	MND	L858R
HP-45863	NOS	MND	MND	MND	MND	MND	L858R	MND	MND	MND	MND	MND	L858R
HP-46155	LU	MND	MND	MND	MND	MND	19del	MND	MND	MND	MND	MND	19del
HP-44217	NOS	MND	MND	MND	MND	MND	19del	MND	MND	MND	MND	MND	19del
HP-44217	NOS	MND	MND	MND	MND	MND	19del	MND	MND	MND	MND	MND	19del
HP-46155	LU	MND	MND	MND	MND	MND	19del	MND	MND	MND	MND	MND	19del
HP-29847	CO	MND	MND	E545K	MND	G12A	MND	MND	MND	E545K	MND	G12A	MND
HP-30384	CO	MND	MND	MND	MND	MND	MND	MND	MND	MND	MND	MND	MND

MND, mutation not detected.

CO, Adenocarcinoma of Colon.

LU, Adenocarcinoma of Lung.

NOS, Not otherwise specified.

_a, Insufficient DNA to complete analysis.

doi:10.1371/journal.pone.0051153.t007

discrepant sample HP-45416 (lung) was not tested for the *EGFR T790M* mutation as the Qiagen DxS assays did not carry the *T790M* assay at the time of the study, and retesting is not possible due to lack of additional sample material.

Sample Input Titrations

In order to confirm the reproducibility and consistency of the methodology, sample input titrations were carried out. To define the effective DNA input concentration over which the assay could be considered accurate, and identify the wild-type and mutant C_T values for each gene, DNA input was varied for plasmids, cell lines, and FFPE samples, with sample preamplification (Table 8). The

C_T values for both the mutant and wild-type show the expected response to input concentration over the titration range.

Platform Reproducibility Validation

The reproducibility of data from mutation detection assays was also evaluated by the comparison of duplicate experiments. The inter- and intra-chip variability in assay C_T values was assessed as shown in figure 2. A total of 5664 duplicate pairs were mapped on a scatter plot, and the Pearson correlation coefficient (R^2) was calculated. The R^2 values were found to be over 0.99 for FAM as well as VIC channels, indicating excellent inter- and intra-chip reproducibility of data generated by the assay.

Table 8. Sample Input Titrations: Effect on Assay Performance.

Plasmid DNA	Mutation Status	Fg Plasmid	Wild-type C _T	Mutant C _T
Plasmid #1	Pk_E542K	100	30	12.28
		10	30	15.71
		1	30	18.55
Plasmid #2	Pk_E545K	100	30	13.23
		10	30	16.23
		1	30	19.98
Plasmid #3	Pk_H1047R	100	30	11.02
		10	30	15.33
		1	30	19.12
Plasmid #4	Pk_H1047L	100	30	13.63
		10	30	17.50
		1	30	21.37

FFPE DNA	Mutation Status	DNA (ng)	Wild-type C _T	Mutant C _T	ΔC _T
HP-30770	Kr_G12R	160	10.66	15.87	5.21
		40	12.66	17.88	5.23
		10	14.48	19.99	5.51
HP-30630	Pk_E542K	160	14.81	15.21	0.40
		40	16.64	16.68	0.04
		10	18.60	18.93	0.33

Cell Line DNA	Mutation Status	DNA (ng)	Wild-type C _T	Mutant C _T	ΔC _T
MGH-U3	Ak_E17K	120	12.01	11.44	-0.57
		15	15.23	15.17	-0.06

doi:10.1371/journal.pone.0051153.t008

Discussion

The future of oncology biomarker detection can be delivered by many promising technologies, including multiplexed protein assays, and parallel next-generation genome sequencing [22,23]. The limited maturity of many of these techniques, combined with their timescale and infrastructure demands, means that there is an unmet need for robust high-throughput biomarker detection methods in the clinical drug development setting.

Our validation has demonstrated that MUT-MAP offers a means of detecting a wide range of mutations in a panel of therapeutically relevant genes, enabling the detection of predictive and prognostic biomarkers from very small amounts of sample DNA. A cross-reactivity analysis showed that this platform has the ability to reliably discriminate between closely related mutations. In addition, the ability of the assay to provide robust reproducible data has been validated in both cancer cell lines and FFPE biopsy samples using considerably smaller amounts of sample DNA than traditional assays. Such an approach enables the study of a wide range of oncogenic mutations in precious clinical samples with very little tissue available for analysis.

As mutations previously thought to be unique to particular tumor types have been shown to be present across a range of cancers (Sanger COSMIC database [24]), the six-gene sample panel used here could be applied to multiple clinical and preclinical studies. The parallel detection of multiple mutations in a single sample also supports

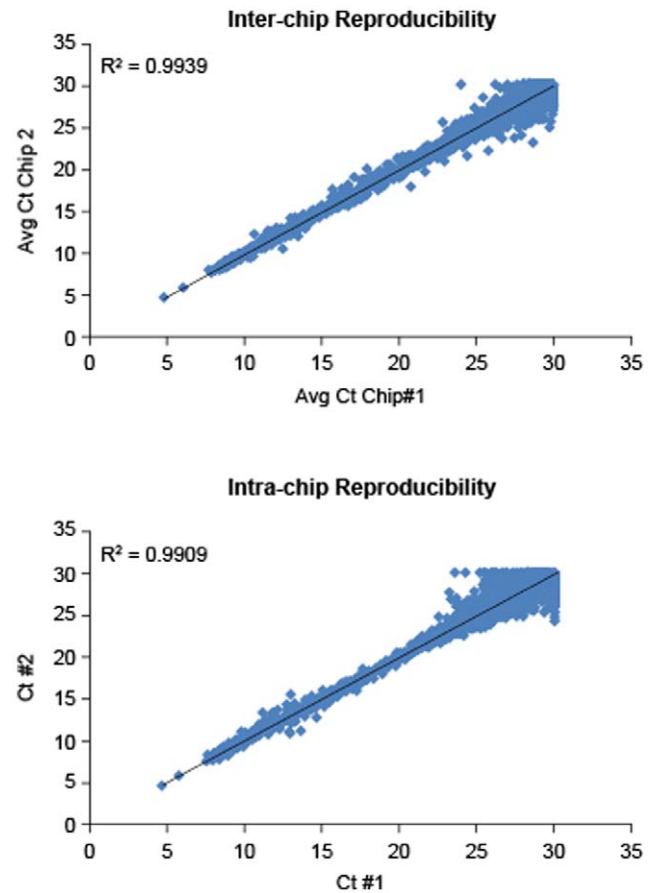


Figure 2. Inter- and Intra-Chip Reproducibility Titrations. The MUT-MAP panel qPCR assays were run in duplicate and C_T outputs were plotted to determine both inter- and intra-chip reproducibility. Data for a typical mutation panel run are shown, with R² correlations of 0.9939 and 0.9909 for inter- and intra-chip reproducibility, respectively. doi:10.1371/journal.pone.0051153.g002

biomarker development for combination treatment regimens, where previous analyses would have taken place independently. Parallel analysis also removes the need for sample tracking over multiple assays, which arises with traditional screening methods. The process is further optimized for clinical research and clinical trials by the availability of commercial kit components, facilitating adaptation of this technique to select patients for experimental therapeutic regimens based on gene mutation biomarker combinations which are identified using the multiplex approach.

In addition to biomarker mapping in the clinical setting, MUT-MAP will enable the retrospective analysis of stored FFPE samples, allowing additional data to be obtained from previous studies and possibly identifying previously unknown biomarker associations. The AS-PCR component of the assay uses proprietary primer modifications and an enzyme screened for improved mismatch discrimination. This enables the high level of sensitivity demonstrated in our study and allows us to multiplex allele-specific assays. This sensitivity enables the accurate and reliable identification of mutation status in multiple genes, from poor-quality, low-mass, preserved clinical samples, thereby allowing the maximum amount of data to be obtained from each sample, and repeat experiments to be conducted from the same biopsy. This capability has exciting potential for the future study of low-yield exploratory biomarkers such as circulating tumor DNA [25]. This highly flexible platform can be used to detect mutations beyond the six genes included in this study; in addition, the precise quantification of

each amplicon opens up the possibility of being able to detect copy number variations. Most significantly, however, the MUT-MAP assay can form the basis for the development of a platform to support efficient biomarker discovery and validation in support of detection and personalized healthcare.

Supporting Information

Table S1 Preamplification Primer Sequences. (DOCX)

References

1. Wistuba II, Gelovani JG, Jacoby JJ, Davis SE, Herbst RS (2011) Methodological and practical challenges for personalized cancer therapies. *Nat Rev Clin Oncol* 8: 135–141.
2. Sawyers CL (2008) The cancer biomarker problem. *Nature* 452: 548–552.
3. ODwyer D, Ralton LD, O'Shea A, Murray GI (2011) The proteomics of colorectal cancer: identification of a protein signature associated with prognosis. *PLoS ONE* 6: e27718.
4. Denkert C, Sinn BV, Issa Y, Maria MB, Maisch A, et al. (2011) Prediction of response to neoadjuvant chemotherapy: New biomarker approaches and concepts. *Breast Care (Basel)* 6: 265–272.
5. Prat A, Ellis MJ, Perou CM (2011) Practical implications of gene-expression-based assays for breast oncologists. *Nat Rev Clin Oncol* 9: 48–57.
6. Jakobsen JN, Sorensen JB (2011) Intratumor heterogeneity and chemotherapy-induced changes in EGFR status in non-small cell lung cancer. *Cancer Chemother Pharmacol* 68: 1–15.
7. Weberpals JI, Koti M, Squire JA (2011) Targeting genetic and epigenetic alterations in the treatment of serous ovarian cancer. *Cancer Genet* 204: 525–535.
8. Mittempergher L, de Ronde JJ, Nicuwlund M, Kerkhoven RM, Simon I, et al. (2011) Gene expression profiles from formalin fixed paraffin embedded breast cancer tissue are largely comparable to fresh frozen matched tissue. *PLoS ONE* 6: e17163.
9. Kuan CT, Wikstrand CJ, Bigner DD (2001) EGF mutant receptor vIII as a molecular target in cancer therapy. *Endocr Relat Cancer* 8: 83–96.
10. Lynch TJ Jr, Bell DW, Sordella R, Gurubhagavatula S, Okimoto RA, et al. (2004) Activating mutations in the epidermal growth factor receptor underlying responsiveness of non-small-cell lung cancer to gefitinib. *N Engl J Med* 350: 2129–2139.
11. Lièvre A, Bachet JB, Le Corre D, Boige V, Landi B, et al. (2006) *KRAS* mutation status is predictive of response to cetuximab therapy in colorectal cancer. *Cancer Res* 66: 3992–3995.
12. Hatzivassiliou G, Song K, Yen I, Brandhuber BJ, Anderson DJ, et al. (2010) RAF inhibitors prime wild-type RAF to activate the MAPK pathway and enhance growth. *Nature* 464: 431–435.
13. Bollag G, Hirth P, Tsai J, Zhang J, Ibrahim PN, et al. (2010) Clinical efficacy of a RAF inhibitor needs broad target blockade in *BRAF*-mutant melanoma. *Nature* 467: 596–599.
14. O'Brien C, Wallin JJ, Sampath D, GuhaThakurta D, Savage H, et al. (2010) Predictive biomarkers of sensitivity to the phosphatidylinositol 3' kinase inhibitor GDC-0941 in breast cancer preclinical models. *Clin Cancer Res* 16: 3670–3683.
15. Holland PM, Abramson RD, Watson R, Gelfand DH (1991) Detection of specific polymerase chain reaction product by utilizing the 5'–3' exonuclease activity of *Thermus aquaticus* DNA polymerase. *Proc Natl Acad Sci U S A* 88: 7276–7280.
16. Shi MM, Myrand SP, Bleavins MR, de la Iglesia FA (2001) Genotyping for Functionally Important Human CYP2D6*4 (B) Mutation Using TaqMan Probes. *Methods Mol Med* 49: 459–472.
17. Newton CR, Graham A, Heptinstall LE, Powell SJ, Summers C, et al. (1989) Analysis of any point mutation in DNA. The amplification refractory mutation system (ARMS). *Nucleic Acids Res* 17: 2503–2516.
18. Okayama H, Curiel DT, Brantly ML, Holmes MD, Crystal RG (1989) Rapid, nonradioactive detection of mutations in the human genome by allele-specific amplification. *J Lab Clin Med* 114: 105–113.
19. Will SG, Tsan A, Newton N (2011) "Allele-Specific Amplification," U.S. Patent 2010/0099110A1. Available: <http://patft.uspto.gov/>. Accessed: 2012 Jul 7.
20. Reichert F, Bauer K, Myers TW, Schoenbrunner NJ, San Filippo J (2012) "DNA polymerases with increased 3'-mismatch discrimination," U.S. Patent 2011/0312041A1; Reichert F, Bauer K, Myers TW, "DNA polymerases with increased 3'-mismatch discrimination," U.S. Patents US 2011-0318785 A1, US-2012-0015405 A1, US-2012-0009628 A1, US 2011-0312037 A1, US 2011-0312039 A1, US 2011-0312038 A1, US 2011-0318786 A1. Available: <http://patft.uspto.gov/>. Accessed: 2012 Jul 7.
21. Forbes SA, Bhamra G, Bamford S, Dawson E, Kok C, et al. (2008) The Catalogue of Somatic Mutations in Cancer (COSMIC). *Curr Protoc Hum Genet* Chapter 10: Unit 11.
22. Mani V, Chikkaveeraiah BV, Rusling JF (2011) Magnetic particles in ultrasensitive biomarker protein measurements for cancer detection and monitoring. *Expert Opin Med Diagn* 5: 381–391.
23. Cronin M, Ross JS (2011) Comprehensive next-generation cancer genome sequencing in the era of targeted therapy and personalized oncology. *Biomark Med* 5: 293–305.
24. Forbes SA, Bindal N, Bamford S, Cole C, Kok CY, et al. (2011) COSMIC: mining complete cancer genomes in the Catalogue of Somatic Mutations in Cancer. *Nucleic Acids Res* 39: D945–D950.
25. Sozzi G, Conte D, Mariani L, Lo VS, Roz L, et al. (2001) Analysis of circulating tumor DNA in plasma at diagnosis and during follow-up of lung cancer patients. *Cancer Res* 61: 4675–4678.

Table S2 TaqMan and Mutation Detection Assays. (DOCX)

Author Contributions

Conceived and designed the experiments: RP. Performed the experiments: RP RD RT. Analyzed the data: RP. Contributed reagents/materials/analysis tools: RP AT RT RD NS TWM KB ES RR. Wrote the paper: RP AT RT RD NS TWM KB ES RR.